geoconvention
Calgary • Canada • June 20-22 2022

Time-lapse VSP detection of a simulated shallow CO_2 leak at the CaMI Field Research Station

Brendan J. Kolkman-Quinn[1], Donald C. Lawton[1,2], Marie Macquet[2]
[1]CREWES, University of Calgary. [2]Carbon Management Canada Containment and Monitoring Institute

Summary

Effective geophysical monitoring is essential for Measurement, Monitoring and Verification (MMV) of geological CO_2 sequestration. The Containment and Monitoring Institute's Field Research Station (CaMI.FRS) near Brooks, Alberta was developed to test monitoring technologies and inform MMV expectations for larger scale operations. CO_2 is currently being injected at 300m depth into the Basal Belly River Sandstone, a brine aquifer of 10% porosity at the base of the Foremost Fm (Dongas, 2016, Macquet and Lawton, 2017). Various geophysical and geochemical monitoring technologies are tested at the FRS, including time-lapse vertical seismic profiles (VSP). Results from CaMI.FRS provide unique field data relevant to shallow-leak detection from Carbon Capture and Storage (CCS) and Enhanced Oil Recovery (EOR) operations in sedimentary basins. VSP data were collected between 2017 and 2021 using geophones and Distributed Acoustic Sensing (DAS). Monitor surveys provided snapshots of the reservoir, with cumulative CO_2 injection amounts of 7 t, 15 t, and 33 t of CO_2. These field data had high repeatability, with permanently installed seismic sensors and repeated shot locations. Seasonally variable surface conditions and near-surface filtering were the main source of dissimilarity between baseline and monitor surveys. The 10 Hz – 150 Hz field data required cautious processing and the development of a reliable, time-lapse compliant workflow. This produced directly comparable amplitudes between baseline and monitor surveys without the need for cross-equalization using shaping filters. Instead, cross-equalization was achieved by applying high-cut filters to match bandwidths between each baseline-monitor shot gather pair. The CO_2 plume was confidently detected and delineated on borehole geophone data after 33 t of injection. Equivalent DAS VSP data yielded ambiguous time-lapse results. The DAS baseline and monitoring data were collected with different interrogators and showed different noise levels. Compared to the high SNR geophone data, the raw DAS data required additional data-preparation steps and aggressive de-noising. Only one monitoring line, with the least-noisy baseline data, showed a weak CO_2 time-lapse anomaly similar to, but noisier than, the geophone result. Surpassing the detection threshold between 15 t and 33 t of injected CO_2 appears to represent the limit of detectability for a shallow CO_2 leak in the particular geological setting at the CaMI.FRS. The 33 t detection threshold and the time-lapse compliant workflow provide insight into the challenges and capabilities of reservoir monitoring and shallow leak detection for geological CO_2 sequestration.

Workflow

Establishing a detecting threshold for the subtle effects of a small quantity of CO_2 motivated the development of a reliable time-lapse compliant VSP workflow with few sources of error. This workflow was developed by streamlining and simplifying the standard VSP workflows previously

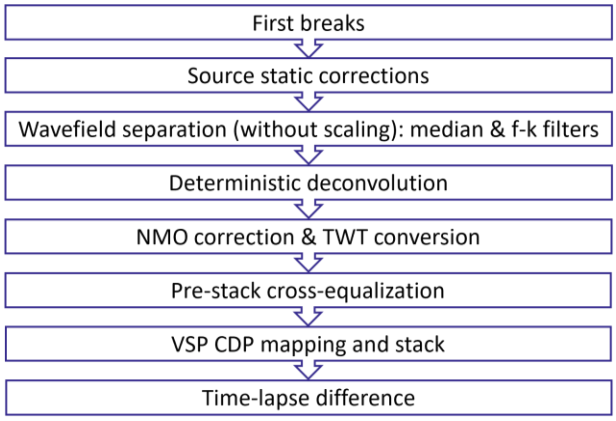

Figure 1. This simplified VSP processing workflow produced highly reliable time-lapse results.

employed at the FRS by Kolkman-Quinn and Lawton (2020) and Gordon (2019). Those had been based on Hinds and Kuzmiski (1996) and the recommended workflows from Schlumberger's VISTA processing software. Figure 1 shows a flow-chart of the simplified time-lapse compliant processing workflow. A detailed explanation of the workflow is given by Kolkman-Quinn (2022). Numerous processing steps were eliminated for being either unnecessary or for being sources of error which had caused dissimilarity between baseline and monitor data. Of note, 3-component data rotation was negatively affected by a series of dead traces in the horizontal components. This required interpolation and risked the introduction of unnecessary error. Thus, processing was performed using only the vertical components of the geophones. This simple 1-C workflow was also directly applicable to straight-fiber DAS data. With successful results from the 1-C workflow achieved, re-introducing the 3-C data will be attempted in the future. Similar to a zero-offset VSP processing flow, wavefield separation was achieved with a median filter and f-k filter, rather than 3-C rotation and time variant wavefield separation. No trace scaling was applied during wavefield separation. Instead, processing relied heavily on deterministic deconvolution to properly scale the trace amplitudes across most of the available frequency bandwidth. This produced directly comparable baseline and monitor reflection amplitudes.

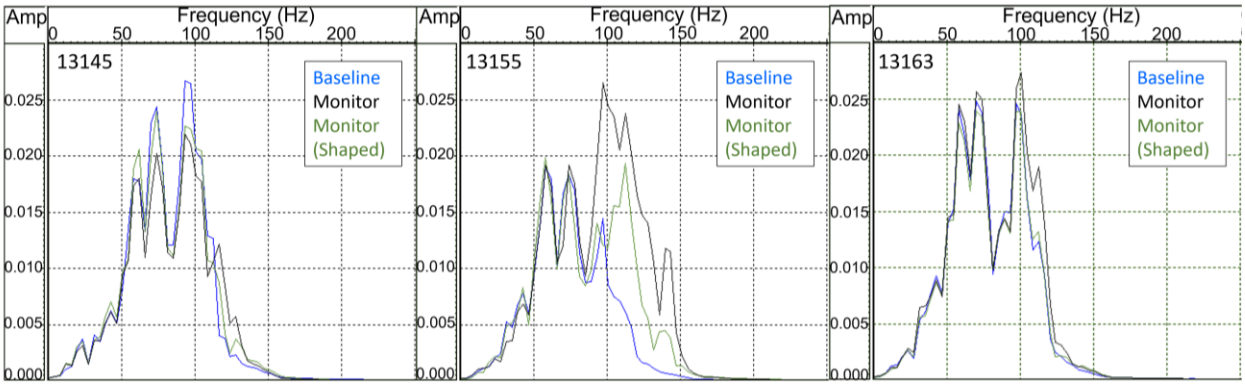

Figure 2. Three examples of shot gather spectra from baseline (blue) and monitor (black) processed shot gathers. Deterministic deconvolution scaled the amplitudes such that they were comparably up to a point of divergence, at which effects of seasonal near-surface filtering were not fully reversed. Shaping filters addressed minor disparities in frequency content, but not major ones such as in shot 13155 (green spectra).

Cross-equalization between baseline and monitor reflection data was principally required to reconcile spectral differences caused by seasonal variations in near-surface filtering. These affected each shot location and shot gather differently, introducing differences in the higher frequency bands which could not be entirely reversed by deterministic deconvolution (Figure 2). The processed reflection data frequency spectra in Figure 2 were taken from a 400 ms window which included the BBRS injection interval. Shaping filters designed from both the downgoing direct arrivals and the upgoing reflected arrivals were tested. Shaping filters designed from upgoing reflection data were found to needlessly influence the BBRS reflection and diminish the time-lapse anomaly, while inadequately matching the highest frequency bands (Figure 2). This produced high-frequency time-lapse residuals from the most mis-matched shot gathers. Shaping filters designed from the downgoing direct arrivals were independent of the reflection data and did not unduly affect the reflection amplitudes. However, those filters were insensitive to severely attenuated higher frequency bands, and failed to adequately address the variable near-surface filtering problem.

Rather than use a shaping filter for cross-equalization, high-cut filters were developed for each baseline-monitor shot gather pair to simply remove the remaining effects of variable near-surface filtering from the otherwise directly comparable baseline and monitor data. This required a shot-by-shot inspection of amplitude spectra, in a manual process that could be automated for larger datasets. The high-cut filtered spectra are shown in Figure 3. With the unresolved seasonal near-surface filtering effects removed from the spectra, the bandwidths matched and the stacked baseline reflection amplitudes could be directly subtracted from the monitor data without need of further cross-equalization. In Figure 3, shot 13145 reflected off the CO_2 plume and its spectrum shows an amplitude difference attributed to CO_2 saturation. This amplitude decrease contributes to a time-lapse anomaly in the difference between baseline and monitor VSP CDP stacked data.

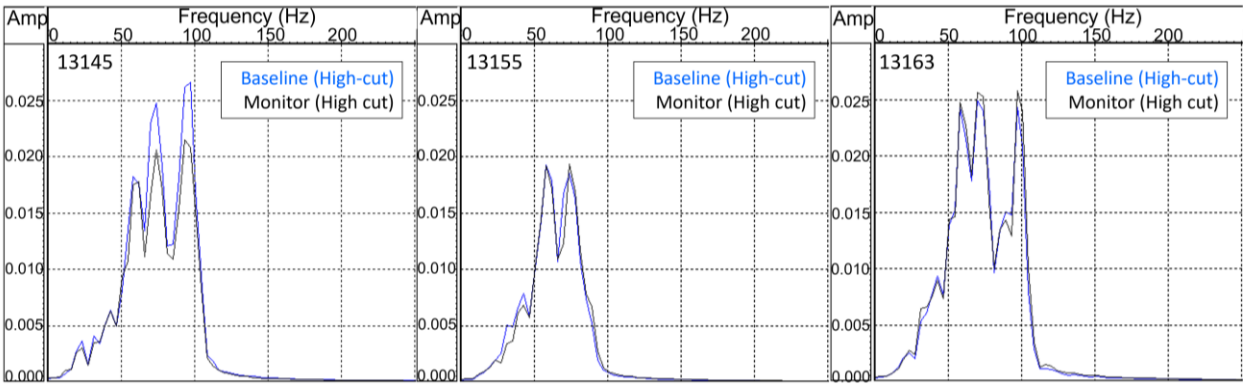

Figure 3. High-cut filtering after deconvolution trimmed the baseline and monitor spectra to a common bandwidth. Shot 13145 reflected off the CO_2 plume and the corresponding amplitude reduction is visible in the monitor spectrum (black) compared to the baseline (blue).

Results and Conclusions

A finite difference VSP forward model set expectations of the plume's signature and extent in a VSP CDP stacked section (Figure 4). The geophysics observation well (Obs 2) is offset 20 m to the south-west from the injection well (Inj). With reservoir porosities of 10% and lower, partial

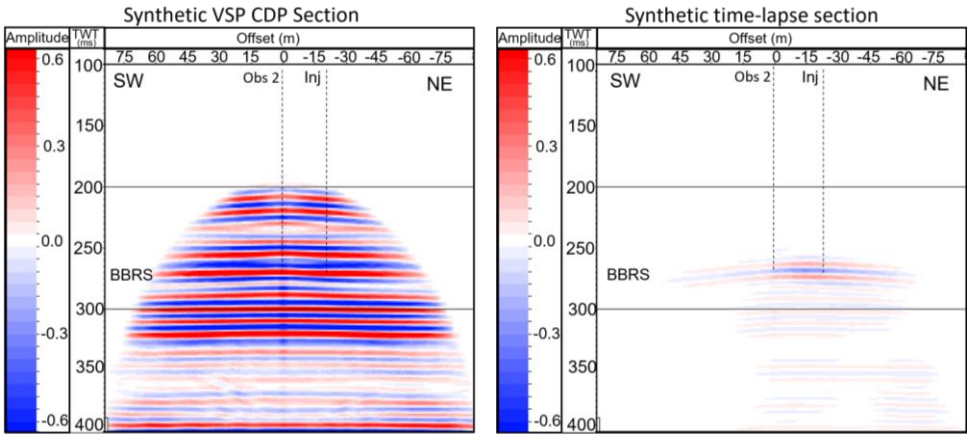

Figure 4. Forward model of the CO_2 anomaly in the BBRS interval, from a finite difference VSP model. The anomaly is a trough-peak succession with side-lobe energy, followed by a weaker anomaly caused by travel-time delay in the monitor data.

saturation of gas-phase CO_2 in the BBRS reservoir causes a gradual decrease in P-wave velocity (Macquet et al., 2019). This produces a trough-peak seismic anomaly with side-lobe energy at the top and bottom of the BBRS reservoir. Following the reflection anomaly, a weaker time-lapse anomaly is caused by travel-time delay through the reservoir in the monitor survey.

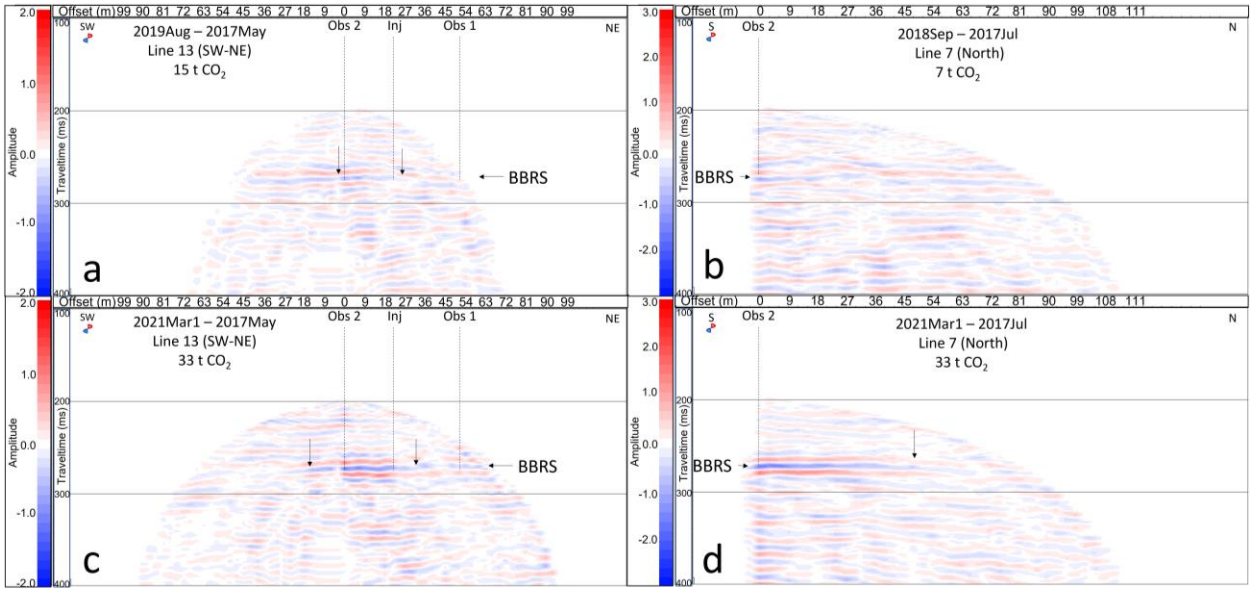

Figure 5. Time-lapse differences of VSP CDP stacked data from CaMI.FRS. Arrows indicate interpreted extent of the CO_2 plume. The 7 t plume had not extended to the north monitoring line by 2018 (b). The Line 13 2019 monitoring survey (a) did not unequivocally detect the 15 t CO_2 plume around the Injection well. A total CO_2 injection amount of 33 t caused unambiguous time-lapse anomalies on both monitoring lines by March, 2021 (c & d).

After applying high-cut filters to match the bandwidths between each baseline and monitor shot gather pair, the stacked baseline data were subtracted from the monitor data to produce a time-lapse difference. Figure 5 shows field data examples of the time-lapse results from two of the principal monitoring lines at CaMI.FRS. Figures 5a & 5b show 1-year and 2-year time-lapse differences corresponding to 7 t and 15 t of injected CO_2. Figures 5b & 5d shows only half of a full walk-away VSP CDP survey, as only the northern half of that line was acquired for that particular monitoring survey. The southern half will be available for future results. In addition, the 2019 monitor survey for Figure 5a had a more limited range of shot offsets, hence the reduced coverage in Figure 5a compared to 5c.

While the 15t CO_2 plume was interpreted in Figure 5a was interpreted, it was not confidently above the detection threshold. Without knowing where to look, the weak effects of the CO_2 saturation would not have been easily distinguished from the background time-lapse residuals in an unexpected shallow leak scenario. In Figures 5c and 5d, the 33 t CO_2 plume had achieved sufficient saturation and extent in the BBRS reservoir to produce clear time-lapse anomalies above the level of the background residuals. These geophone results indicate that the plume's detection threshold was surpassed between 15 t and 33 t of injection. The detection threshold is a product of both the CO_2 saturation and the lateral extent of the plume, which in this case is approximately 50 m for the 33 t injection amount. Inversion of the baseline and monitor data will be performed in the future, to better characterize the CO_2 saturations necessary to detect the CO_2 plume.

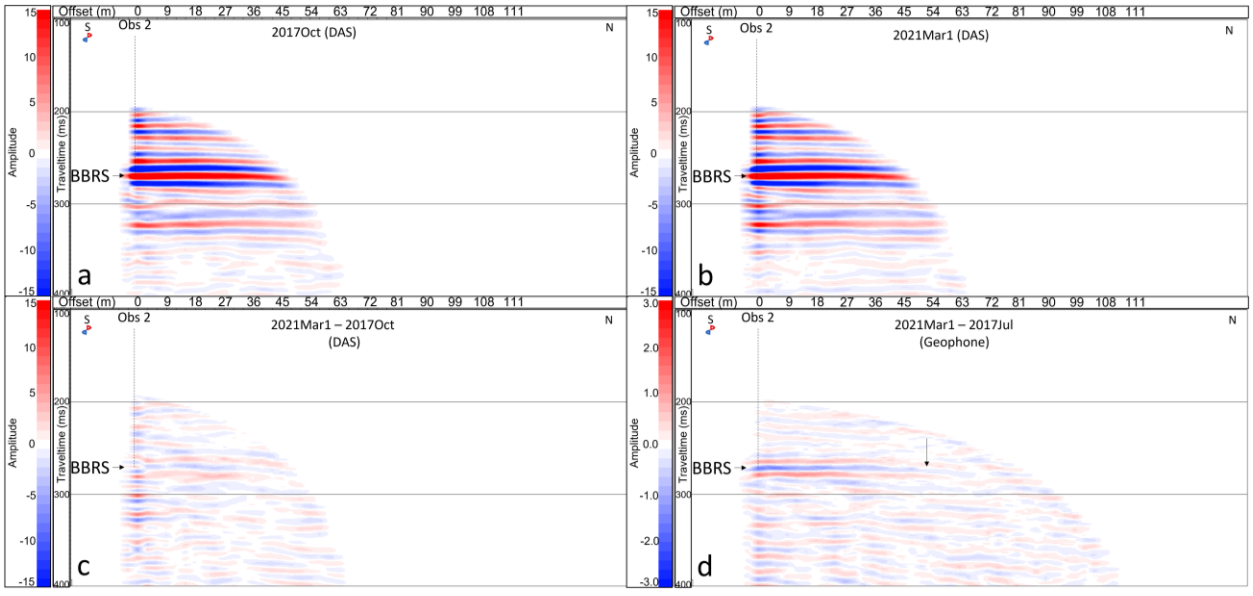

Figure 6. Line 7 DAS baseline (a) and monitor (b) VSP CDP stacks and time-lapse difference (c). For this display, DAS trace depths were trimmed to 190 m-305 m to be equivalent to the geophone depths. The DAS baseline was limited to 150 m shot offsets, allowing less coverage than the geophone data. The CO_2 anomaly in the geophone data (d) is not as pronounced in the DAS data (c).

Although the 1-C time-lapse workflow could be directly applied to the straight-fiber DAS data available at CaMI.FRS, additional processing steps were required: spatial re-sampling, depth-registration, and aggressive de-noising of the raw DAS data (Kolkman-Quinn, 2022). The time-lapse result from the best quality DAS data is shown in Figure 6. The reduced lateral coverage is due to the DAS baseline data only extending to 150 m shot offset. Unlike the geophone data, the DAS time-lapse result is ambiguous. In Figure 6c, there is a weak time-lapse anomaly at the BBRS interval which does not clearly stand out from the background time-lapse residuals. Interrogator-related noise in the raw DAS data were found to cause dissimilarity between pairs of baseline and monitor shot gathers. Despite aggressive de-noising of the raw data using f-k and median filters (Kolkman-Quinn, 2022), it was determined that noise in the raw DAS data negatively affected the subtraction of baseline from monitor data. Unlike the geophone result in Figure 6d, the DAS-related noise prevented the CO_2 anomaly from clearly showing through in the stacked results. Future monitoring data will determine whether increased CO_2 saturation in the reservoir will allow for a higher detection threshold to be established for the DAS data, or if further work on DAS de-noising must be attempted.

The successful detection of 33 t of CO_2 in the 300 m deep sandstone reservoir of up to 10% porosity demonstrates the MMV capabilities and limitations of time-lapse VSPs. These results were achieved with high quality monitoring data and cautious processing, pushing the limit of detectability in this geological setting. The workflow and detection threshold help inform MMV expectations for both shallow leak detection and shallow reservoir monitoring of CO_2 sequestration operations.

Acknowledgements

Thanks to Kevin Hall, Kevin Bertram, and Malcolm Bertram from CREWES for acquiring the field data. We would like to thank the sponsors of CREWES and CaMI for their continued support. This work was funded by CREWES industrial sponsors and NSERC (Natural Science and Engineering Research Council of Canada) through the grant CRDPJ 543578-19. The data were acquired through a collaboration with the Containment and Monitoring Institute (CaMI) of Carbon Management Canada (CMC). Research at the CaMI field site is supported by the Canada First Research Excellence Fund, through the Global Research Initiative at the University of Calgary.

References

Dongas, J., 2016, Development and characterization of a geostatic model for monitoring shallow CO_2 injection: M.Sc. Thesis, University of Calgary.

Gordon, A., 2019, Processing of DAS and geophone VSP data from the CaMI Field Research Station: M.Sc. Thesis, University of Calgary.

Hinds, R.C., Anderson, N.L., and Kuzmiski, R.D., 1996, VSP Interpretive Processing: Theory and Practice: Society of Exploration Geophysics.

Macquet, M., Lawton, D., 2017, Reservoir simulations and feasibility study for seismic monitoring at CaMI.FRS: CREWES Research Report, **29**, 56.1-56.26.

Macquet, M., Lawton, D., Saeedfar, A., Osadetz, K., 2019, A feasibility study for detection thresholds of CO_2 at shallow depths at the CaMI Field Research Station, Newell County, Alberta, Canada: Petroleum Geoscience, **25**, 509-518.

Kolkman-Quinn, B., 2022, Time-lapse VSP monitoring of CO2 sequestration at the CaMI Field Research Station: M.Sc. Thesis, University of Calgary.